

Peripheral Arylation of Subporphyrazines

Tomohiro Higashino,^[a, b] M. Salomé Rodríguez-Morgade,^{*[a]} Atsuhiko Osuka,^{*[b]} and Tomás Torres^{*[a, c]}

Abstract: Peripherally hexaarylated subporphyrazines (SubPzs) have been prepared through a Pd-catalyzed, CuTC-mediated coupling of a hexaethylsulfanylated subporphyrazine with arylboronic acids. The introduced aryl substituents strongly influence the electronic properties of the subporphyrazine through effective conjugative interaction. Aryl rings endowed with π -electron-donating groups at the *para*

positions produce a remarkable perturbation of the electron density of the SubPz macrocycle. This is reflected through significant redshifts of the SubPz CT and Q-bands, together with increase of the molar absorptivity of

the former, with respect to those exhibited by the hexaphenyl-SubPz **2a**. Moreover, the trend in the first SubPz reduction potentials correlates with the Hammett constants (σ_p) corresponding to the *para* substituents of the aryl. The domed, extended SubPz π -system self-assembles in the solid state to form a dimeric capsule that houses a solvent molecule.

Keywords: arylation • conjugation • cross-coupling • electrochemistry • porphyrins

Introduction

Subporphyrazines (SubPz) are aromatic porphyrinoids consisting of three pyrrole subunits connected through their 2,5-positions by aza bridges.^[1] Structurally, they arise from the formal removal of the three benzene rings from subphthalocyanines (SubPcs)^[2] and hence, they share some properties with SubPcs. For example, SubPzs exist only as boron(III) complexes. In addition, they show great potential as functional chromophores owing to their strong fluorescence and their cone-shaped, aromatic structure arising from a 14π -electron circuit. As a distinctive feature, SubPzs strongly absorb in the green-yellow regions.^[3]

Unlike the extensively studied chemistry of SubPcs, that of SubPzs remains mostly unexplored, mainly due to the limited synthetic methodology for the construction of the

SubPz macrocycle. So far, SubPzs have been prepared by boron(III)-assisted cyclotrimetrization of maleonitrile derivatives. For this reaction, the stereochemistry of the dinitrile precursor has proven crucial. In fact, neither bis(alkyl)- or bis(aryl)fumaronitriles afford SubPzs under the standard reaction conditions.^[1a] The only exception has been the use of unsubstituted fumaronitrile in a mixed condensation with tetramethylsuccinonitrile. This gave a mixture of a subazachlorin and unsubstituted SubPz.^[4] Unfortunately, chemical manipulation of unsubstituted SubPz is not feasible due to its proven instability once formed.^[4] Finally, the use of boron trichloride is incompatible with many functions, in particular, with precursors bearing boron-coordinating heteroatoms such as nitrogen or even oxygen. These synthetic limitations have precluded the development of a variety of SubPz derivatives, parallel to those reported for the SubPc^[2] and subporphyrin (SubP)^[5,6] series.

SubPzs represent far more than just SubPc derivatives lacking the fused benzene rings, but they are rather a distinctive class of porphyrinoids. This is true because in these series, the peripheral substituents are directly attached to the macrocyclic core. Hence, these functions exert much stronger influence on the aromatic heteroannulene, related to their SubPc congeners, whose peripheral substituents are appended to the fused benzene rings. A typical example is hexaethylsulfanyl-substituted SubPz **1**, which exhibits a very strong and broad charge-transfer band at 438 nm (the strongest absorption of the spectrum) and a bathochromically shifted (60 nm) and broad Q-band at about 560 nm. These striking electronic alterations upon peripheral thioalkyl substitution arise from π -donation from the sulfur lone pair to the SubPz core. The spectral changes are about twofold larger than that produced in SubPcs. Despite this potential, there have been only limited examples of peripherally sub-

[a] T. Higashino, Dr. M. S. Rodríguez-Morgade, Prof. T. Torres
Departamento de Química Orgánica
Universidad Autónoma de Madrid
Cantoblanco, 28049 Madrid (Spain)
Fax: (+34) 914973966
E-mail: salome.rodriguez@uam.es
tomas.torres@uam.es

[b] T. Higashino, Prof. Dr. A. Osuka
Department of Chemistry
Graduate School of Science, Kyoto University, Sakyo-ku
Kyoto 606-8502 (Japan)
Fax: (+81) 75-753-3970
E-mail: osuka@kuchem.kyoto-u.ac.jp

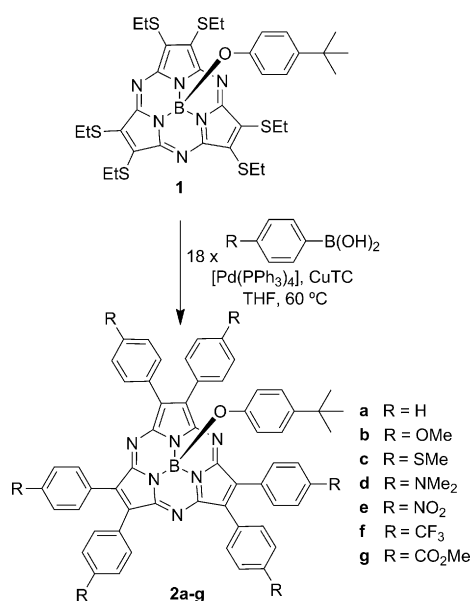
[c] Prof. T. Torres
IMDEA-Nanociencia, c/Faraday, 9, Campus de Cantoblanco
28049 Madrid (Spain)

Supporting Information for this article is available on the WWW under <http://dx.doi.org/10.1002/chem.201301140>.

stituted SubPzs.^[1a,c,3,7] Bearing this in mind, we envisaged peripheral functionalization of SubPzs as a powerful tool to obtain dyes exhibiting exceptional optical and redox properties. Herein, we report the effective peripheral arylation of SubPzs by Pd-catalyzed cross-coupling reaction of hexaethylsulfanyl-substituted SubPz **1** with arylboronic acids. As expected, the newly synthesized hexaaryl-substituted SubPzs show electronic properties far beyond what is usually accessible within the SubPc and SubP families. The use of such a convergent synthetic protocol is unprecedented within porphyrin chemistry and represents the first peripheral modification of preformed SubPzs.^[8]

Results and Discussion

Synthesis: We have applied the methodology developed by Liebeskind and Srogl consisting in the palladium-catalyzed, copper(I) thiophene-2-carboxylate (CuTC)-mediated coupling of boronic acids with heteroaromatic thioethers.^[9] The SubPz precursor was provided with a *tert*-butylphenoxy group at the axial position to guarantee solubility of intermediates and products in organic solvents. The SubPz **1** (Scheme 1) was easily synthesized in 14% yield by using reported procedures,^[1,10] and used in all the cross-coupling reactions as the heteroaromatic reactant.



Scheme 1. The synthesis of hexaaryl-SubPzs.

The CuTC-mediated cross-coupling reaction of **1** with a variety of arylboronic acids at 60 °C afforded the hexaaryl-substituted-SubPzs **2a-g** in 20–43% yields (Scheme 1). In most cases, the six-fold coupling proceeded smoothly for 20 h, using three equivalents of arylboronic acid and CuTC, and 10% mol of palladium catalyst per thioether unit. An exception was found with **2d**, which was obtained in only 3% yield by using our standard protocol. In this case, the yield

was improved up to 23% by performing the reaction at room temperature, although a longer reaction time was required (5 days).

Hexaaryl-substituted SubPzs **2a-g** were characterized by MS, ¹H, ¹³C, and ¹¹B NMR spectroscopies (see the Supporting Information), as well as UV/Vis and fluorescence spectroscopies. The redox properties of **2a-g** were also studied by cyclic voltammetry (CV) and differential pulse voltammetry (DPV). In addition, relevant information about the molecular structure of hexaaryl-substituted-SubPzs was obtained from X-ray diffraction analysis of suitable single crystals obtained for **2b**.

The ¹H NMR spectrum of hexaphenyl-SubPz **2a** exhibits the aromatic protons corresponding to the axial *tert*-butylphenoxy substituent quite shielded (Figure S3a, the Supporting Information), owing to the diatropic ring-current of the 14 π -electron SubPz core. Importantly, the peripheral phenyl rings appear as a single set of two signals, suggesting free rotation of the phenyl rings. Taking into account the SubPz cone-shape, restricted rotation of the peripheral substituents would split each signal in two.^[11,12] The same conclusion can be inferred from the ¹H NMR spectra of all the other hexaaryl-SubPzs **2b-g** (Figure S4a–S9a in the Supporting Information).

Optical properties: Contrasting with what was observed for the hexaaryl-substituted SubPc series,^[13] the peripheral aryl groups of hexaaryl-SubPzs **2a-g** strongly interact with the macrocyclic core. This becomes very apparent when analyzing the optical spectra of these compounds (Figure 1 and Table 1).

Table 1. Optical properties of SubPzs in CHCl₃.

| SubPz | Absorption λ [nm] (ϵ [10^4 M ⁻¹ cm ⁻¹]) | Fluorescence λ_{em} [nm] ^[a] |
|---------------------------------------|--|--|
| Pr ₆ SubPz ^[1c] | 291 (3.8), 329 (sh), 499 (4.0) | 520 |
| 1 | 282 (2.4), 438 (2.7), 556 (2.4) | 682 |
| 2a | 250 (4.4), 304 (4.0), 395 (3.2), 539 (5.2) | 563 |
| 2b | 271 (5.9), 434 (3.9), 553 (4.4) | 612 |
| 2c | 287 (8.7), 454 (4.5), 560 (5.0) | 654 |
| 2d | 296 (9.3), 503 (5.3), 570 (4.2) | 765 |
| 2e | 297 (6.1), 386 (3.4), 547 (5.7) | 581 |
| 2f | 252 (4.7), 308 (4.3), 384 (3.0), 538 (5.7) | 564 |
| 2g | 276 (6.8), 312 (5.0), 394 (3.4), 545 (5.8) | 574 |

[a] Excited at the Q-band.

Thus, hexaarylation of SubPc produces a redshift in the Q-band of the macrocycle of only 5–10 nm with respect to the hexaalkylated derivative.^[13,14] However, hexaphenyl-SubPz **2a** shows the corresponding Q-band at 539 nm (Figure 1b), that is, bathochromically shifted 40 nm with respect to the hexaalkylated SubPz (Table 1).^[1a] However, the most remarkable feature in the absorption spectrum of **2a** is the presence of an intense charge-transfer absorption at 395 nm, which is diagnostic of electronic communication between the phenyl rings and the SubPz macrocycle. Such a CT band does not appear in the electronic spectrum of hexaaryl-SubPcs.^[13]

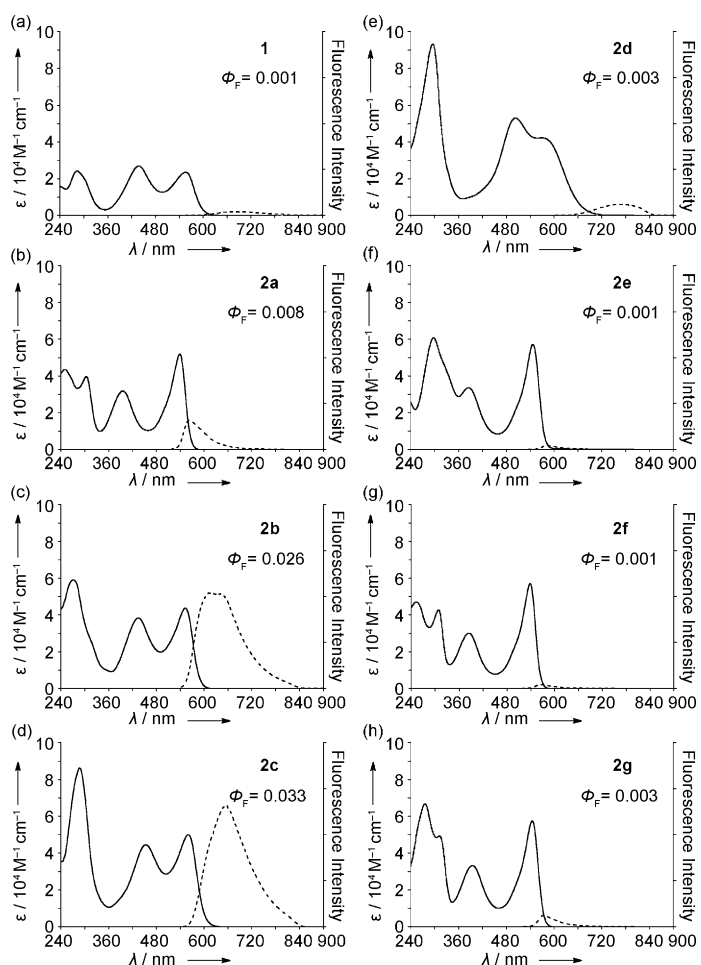


Figure 1. UV/Vis absorption (—) and emission (-----) spectra of (a) **1**, (b) **2a**, (c) **2b**, (d) **2c**, (e) **2d**, (f) **2e**, (g) **2f**, and (h) **2g** in CHCl_3 .

Notably, the redshift of the SubPz Q-band is quantitatively comparable to that produced upon peripheral arylation of porphyrazines (Pz).^[15] The charge-transfer band, however, is exceedingly more intense in the SubPz class than in the Pz series.^[15]

Importantly, the electronic properties of hexaaryl-SubPzs can be fine-tuned by introducing groups of distinct nature at the *para* positions of the peripheral aryl groups (see Figure 1 and Table 1). Here, the effects are different depending on the electron donor or acceptor abilities of the *para* substituents. SubPzs **2b–d** bearing π -electron-donating substituents display Q-bands considerably redshifted with respect to the hexaphenyl-SubPz **2a**. The largest effect is observed for the dimethylamino-substituted hexaaryl-SubPz **2d**, which shows this absorption at 570 nm. π -Electron-donating substituents also produce an increase in the molar absorptivity of the CT bands and shift these absorptions to the lower-energy side. The extent of both effects follow the order $\text{Me}_2\text{N} > \text{MeS} > \text{MeO}$.

Electron-withdrawing groups produce more modest alterations in the CT and Q-bands of the hexaaryl-SubPzs. In compounds **2e–g** CT absorptions are less intense and shifted

hypsochromically only by 1–11 nm, related to **2a**. On the other hand, whereas the π -electron-accepting nitro- and carboxy groups produce a slight redshift of 6–8 nm in the Q-bands, SubPz **2f**, substituted with the σ -electron-accepting CF_3 group, exhibits this band at the same energy as **2a**.

Visible-light excitation in the 510–570 nm range (Q-bands of **1** and **2a–g**) generates different fluorescence patterns depending on the SubPz peripheral substitution. Except for **2b** and **2c**, hexaaryl-SubPzs display fluorescence spectra that look like virtual mirror images to the absorption (Figure 1, dotted lines).

For SubPzs **2b** and **2c** bearing *para*-methoxy and *para*-methylsulfanyl groups, respectively, at the peripheral phenyl rings, the emission bands broaden. The Stokes shifts in hexaalkyl-^[1c] and hexaphenyl-SubPzs are in the similar range (21–26 nm). Electron-donating groups increase this value in the order NMe_2 (195 nm) $>$ MeS (94 nm) $>$ MeO (59 nm). The differences in the quantum yields are also notable. Thus, whereas **2a,d,e,f**, and **g** show low quantum yields (0.001–0.008) in the same range as the SubPz **1**, functionalization with methoxy and methylsulfanyl-substituents in **2b** and **2c** induces much stronger emissions (0.026–0.033).

X-ray crystallography: The optical properties of hexaaryl-SubPzs can be rationalized taking into account their molecular structure. Single crystals of **2b** suitable for X-ray diffraction analysis were obtained by vapor diffusion of octane into a solution of this SubPz in 1,2-dichloroethane. The crystal structure^[16] (Figure 2a and 2b) revealed the curved SubPz shape with a bowl depth of 1.742 Å, very similar to that of Pr_6SubPz .^[10,12]

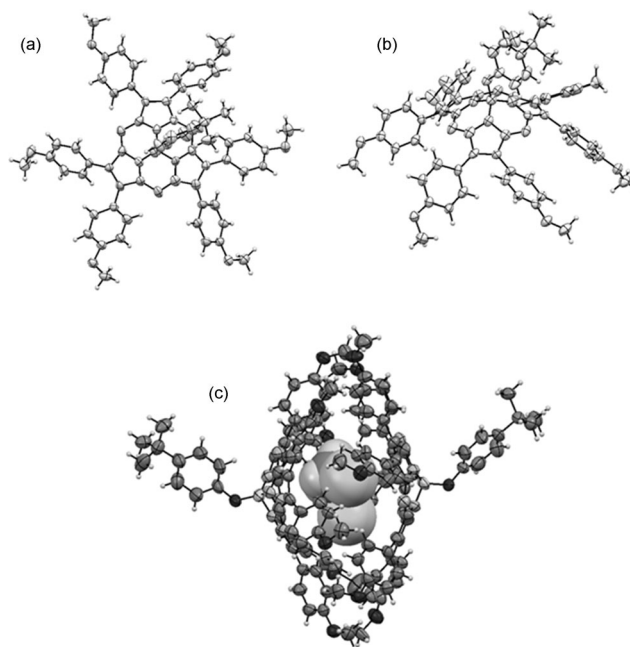


Figure 2. X-ray crystal structure of **2b** (a) top view, (b) side view, and (c) SubPz dimer with the encapsulated solvent, with the thermal ellipsoids drawn at the 50% probability level.

A significant feature of the structure of **2b** is the relatively small dihedral angles of aryl groups with respect to the plane defined by the pyrrole to which they are attached. These small angles, which range from 31.29 to 50.77°, are favorable for π -conjugation over the entire molecule. Remarkably, the dihedral angles of β -phenyl substituents in subporphyrins are much larger, in the 65–82° range. In the latter case, the presence of three additional aryl groups at the SubP *meso*-positions give rise to more congested molecules, with restricted rotation of their peripheral aryl groups.^[17]

To accommodate the six aryl groups in the meager SubPz peripheral space, each benzene ring in a pyrrole unit is tilted by 11–18° with respect to the contiguous benzene ring. The corresponding dihedral angle between two adjacent benzene rings within octaarylporphyrazines is considerably larger (about 55°).^[15b] Overall, the largest dihedral angle between two consecutive benzene rings is of 45.23° for SubPzs and 89.18° for Pzs. The observed free rotation and small dihedral angles of the peripheral aryl substituents in the SubPz class are related to their smaller C_{α} –N– C_{α} angles with respect to that of Pzs (114 vs. 124°), which provide more room for peripheral substituents. Octaphenyl-Pzs are more congested than hexaphenyl-SubPzs and so, the aryl groups are forced to take less coplanar conformations in Pzs, with the consequent mitigation of conjugative effects. This gives rise to stronger influences of the peripheral aryl substituents on the electronic properties of the subporphyrazines related to those of porphyrazines.

Two molecules of **2b** arrange a dimer in the solid state, with the two concave surfaces facing each other and forming a cavity that houses a molecule of 1,2-dichloroethane (Figure 2c). The B–B distance between the SubPz pair is 9.69 Å. One molecule is rotated by 30.34° with respect to the other SubPz, so that the aryl groups are placed in alternated configuration. The O–O distance between two contiguous methoxy groups, that is, one from a SubPz unit and the other one from the other SubPz unit, ranges from 3.87–5.31 Å.

Electrochemistry: The electrochemical properties of hexaaryl-SubPzs **2a–g** were studied by CV (Figure 3) and DPV (Figure S10 in the Supporting Information). Table 1 and Table S1 (the Supporting Information) give the redox potentials derived from these measurements.

SubPzs **1** and **2a–g** exhibit a larger number of redox processes than those exhibited by hexaalkyl-SubPzs.^[12] In particular, whereas the latter show only one reduction and one oxidation peak, all the SubPzs reported in this work display at least three reduction processes that are reversible in most cases, and one or more oxidation peaks that are irreversible for compounds bearing thioether functions (**1** and **2c**). Another interesting feature when comparing hexaalkyl- and hexaphenyl-SubPzs is that **2a** is easier to reduce and more difficult to oxidize. Again, this differs from what has been observed upon peripheral perarylation of Pzs: Octaphenyl-Pzs are more resistant to both electrochemical oxidation and reduction than octaalkyl-Pzs.^[18]

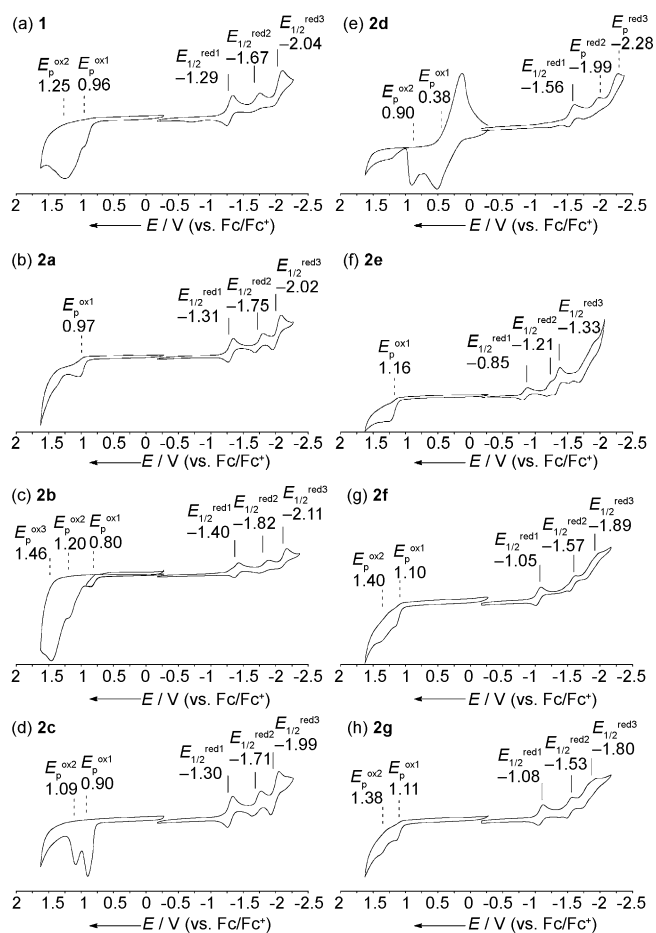


Figure 3. Cyclic voltammograms of (a) **1**, (b) **2a**, (c) **2b**, (d) **2c**, (e) **2d**, (f) **2e**, (g) **2f**, and (h) **2g**. Solvent: CH₂Cl₂; scan rate: 0.05 V s⁻¹; working electrode: glassy carbon; reference electrode: Ag/AgClO₄; electrolyte: Bu₄NPF₆.

The effect of *para* substituents on the redox properties of hexaaryl-SubPzs is remarkable and varies according to the electronic characteristics of the groups. Therefore, six nitro moieties shift the first electrochemical reduction by 460 mV towards more positive potentials (from –1.31 for **2a** to –0.85 V for **2e**), whereas the amino functions of **2d** shift the same process cathodically by 250 mV (Table 2). This is consistent with significant perturbation of the electron density

Table 2. Electrochemical oxidation and reduction potentials, $E_{1/2}$ and E_p versus Fc/Fc⁺ (in V) for the SubPzs studied in this work.

| | E_p^{ox3} | E_p^{ox2} | E_p^{ox1} | $E_{1/2}^{red1}$ | $E_{1/2}^{red2}$ | $E_{1/2}^{red3}$ |
|-----------|----------------------|----------------------|------------------------|------------------|----------------------|----------------------|
| 1 | – | +1.25 ^[a] | +0.96 ^[a] | –1.29 | –1.67 | –2.04 |
| 2a | – | – | +0.97 ^[b] | –1.31 | –1.75 | –2.02 |
| 2b | +1.46 ^[c] | +1.20 ^[a] | +0.80 ^[b] | –1.40 | –1.82 | –2.11 |
| 2c | – | +1.09 ^[a] | +0.90 ^[a] | –1.30 | –1.71 | –1.99 |
| 2d | +0.90 ^[a] | +0.38 ^[b] | +0.22 ^[b,d] | –1.56 | –1.99 ^[a] | –2.28 ^[c] |
| 2e | – | – | +1.16 ^[b] | –0.85 | –1.21 | –1.33 |
| 2f | – | +1.40 ^[c] | +1.10 ^[b] | –1.05 | –1.57 | –1.89 |
| 2g | – | +1.38 ^[c] | +1.11 ^[b] | –1.08 | –1.53 | –1.80 |

[a] Irreversible process (potential corresponds to the peak potential). [b] Taken from the DPV. [c] In the window limit. [d] Multielectronic process.

of the SubPz macrocycle by the *para* substituents of peripheral aryl groups.

The trend in the first reduction potentials correlates with the Hammett constants (σ_p) corresponding to the substituents, so that the potentials are shifted cathodically in the order: $\text{NO}_2 < \text{CF}_3 < \text{CO}_2\text{Me} < \text{H} \approx \text{MeS} < \text{MeO} < \text{NMe}_2$ (Figure 4).^[19]

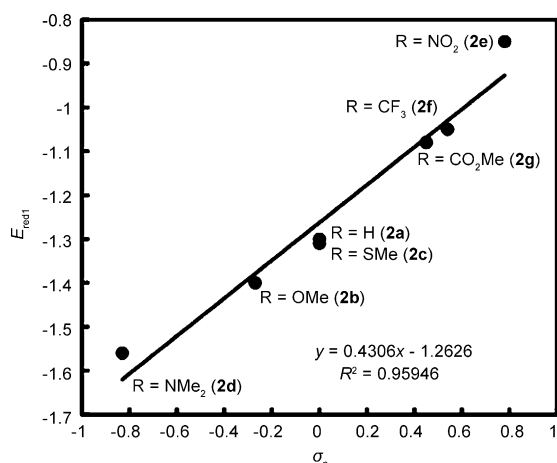


Figure 4. Hammett plot of first reduction potentials of SubPzs **2a–g**.

The oxidation potentials of the macrocycles show less variation across the series (Table 2). The first oxidation process for compounds **2a,b,e,f**, and **g** is partially chemically reversible^[20] (see Figure 3 and S10, the Supporting Information) and is followed by irreversible oxidations afterwards. In agreement with what was expected, the trend correlates quite well with the corresponding Hammett constants for each substituent. Thus, compounds **2e–g** have more positive oxidation potentials than **2a**, whereas **2b** shows a less-positive potential because of their electron-withdrawing or -donating substituents, respectively.

The CV and DPV of **2d** (see Figure S10, the Supporting Information) reveal two additional oxidation processes prior to the oxidation of the SubPz ring. The first oxidation wave consists in several processes involving three electrons, whereas the second wave is a reversible oxidation also involving three electrons. An examination of the redox behavior of aromatic amines suggests that both processes are attributable to the six amino groups.^[21] Separate oxidation processes imply that the *para*-amino substituents communicate with each other in an electrochemical sense through the SubPz core. As a result of the oxidation processes on the amino groups, compound **2d** has a more positive oxidation for the $[\text{SubPz}^1]/[\text{SubPz}^{2-}]$ couple than **2b** (+0.90 and +0.80 V, respectively).

Conclusion

A series of perarylated subporphyrazines has been prepared through a convergent strategy employing a palladium-catalyzed, CuTC-mediated coupling of hexaethylsulfanylated SubPz with arylboronic acids. The ready availability of the bis(thioether)maleonitrile precursors on a multigram scale compensates the low yield for the cyclotrimerization reaction to afford **1** as a precursor. Hexaaryl-SubPzs consist in extended-conjugated systems that display small dihedral angles between the benzene and the pyrrole rings. The introduced aryl substituents exert notable perturbations on the optical and electronic properties of the SubPz core, making these modifications a promising tool to tune SubPzs. The synthetic method provides a useful platform for further symmetric or unsymmetric functionalization of SubPzs, which is actively being pursued in our laboratories.

Experimental Section

Instrumentation and materials: Commercially available solvents and reagents were used without further purification unless otherwise mentioned. Silica-gel column chromatography was performed on Wakogel C-200 or C-300. UV/Vis absorption spectra were recorded with a Shimadzu UV-3100PC spectrometer. Fluorescence spectra were recorded on a Shimadzu RF-5300PC spectrometer. Absolute fluorescence quantum yields were determined on HAMAMATSU C9920-02S. ^1H , ^{13}C , ^{11}B , and ^{19}F NMR spectra were recorded with a JEOL ECA-600 spectrometer (operating at 600 MHz for ^1H , 150 MHz for ^{13}C , 192 MHz for ^{11}B , and 565 MHz for ^{19}F) by using the residual solvent as the internal reference for ^1H (CDCl_3 : $\delta = 7.26$ ppm), the residual solvent as the internal reference for ^{13}C (CDCl_3 : $\delta = 77.16$ ppm), $\text{BF}_3 \cdot \text{Et}_2\text{O}$ as the external reference for ^{11}B ($\delta = 0.00$ ppm), and hexafluorobenzene as the external reference for ^{19}F ($\delta = -162.9$ ppm). Mass spectra were recorded with a BRUKER microTOF LC by using the ESI-TOF method in the positive ion mode in an acetonitrile solution. Single-crystal X-ray diffraction analysis data for compound **2b** was collected at -180°C with a Rigaku R-Axis RAPID II diffraction by using graphite monochromated $\text{Cu}_{\text{K}\alpha}$ radiation ($\lambda = 1.54187 \text{ \AA}$). The structures were solved by using the direct method (SHELXS-97). Redox potentials were measured by the cyclic voltammetry method on an ALS electrochemical analyzer model 660.

Synthesis: The synthetic procedure for CuTC can be found in the Supporting Information.

4-tert-Butylphenoxy[2,3,7,8,12,13-hexa(ethylthio)subporphyrazinato]-boron(III) (1): A 1 M solution of BCl_3 in xylenes (2.0 mL, 2.0 mmol) was added under a N_2 atmosphere to bis(ethylthio)maleonitrile (396 mg, 2.0 mmol) and the mixture was heated at 100°C for 45 min. The solvent was removed under reduced pressure. Then, the residue was dissolved in toluene (4 mL) and 4-tert-butylphenol (1.50 g, 10 mmol) was added. The resulting solution was stirred at reflux for 2 h and afterwards the solvent was evaporated. Column chromatography on silica gel using a 20:1 mixture of *n*-hexane and ethyl acetate gave **1** (70 mg, 14%) as a red syrup. ^1H NMR (600 MHz, CDCl_3): $\delta = 6.82$ (d, $J = 8.6$ Hz, 2H; $\text{H}^{3,5}$), 5.31 (d, $J = 8.6$ Hz, 2H; $\text{H}^{2,6}$), 4.03 (m, 6H; $-\text{SCH}_2\text{CH}_3$), 3.66 (m, 6H; $-\text{SCH}_2\text{CH}_3$), 1.60 (t, $J = 7.2$ Hz, 18H; $-\text{SCH}_2\text{CH}_3$) and 1.14 ppm (s, 9H; *t*Bu); ^{13}C NMR (150 MHz, CDCl_3): $\delta = 154.1$, 150.1, 144.5, 151.6, 125.7, 119.2, 34.0, 31.5, 29.4, 15.8 ppm; ^{11}B NMR (192 MHz, CDCl_3): $\delta = -16.32$ ppm. UV/Vis (CHCl_3): $\lambda(\epsilon) = 282$ (24000), 438 (27000), 556 nm (24000 $\text{M}^{-1}\text{cm}^{-1}$); fluorescence (CHCl_3): $\lambda_{\text{ex}} = 530$ nm; $\lambda_{\text{max}} = 682$ nm; $\Phi_{\text{F}} = 0.001$; HRMS (ESI-TOF, +): m/z calcd for $\text{C}_{34}\text{H}_{44}\text{BN}_6\text{OS}_6$: 755.1995 $[M+\text{H}]^+$; found: 755.1987.

Typical procedure for the cross-coupling of subporphyrazine with boronic acids: An oven-dried flask containing hexa(ethylthio)subporphyrazine **1**

(15.1 mg, 20 mmol; 1 equiv), boronic acid (18 equiv), [Pd(PPh₃)₄] (13.9 mg, 12 mmol; 60 mol %), and CuTC (68.6 mg, 360 mmol; 18 equiv) was purged with N₂, then charged with dry THF (2 mL). The mixture was stirred at 60 °C for 20 h under N₂ atmosphere. The reaction mixture was cooled to room temperature and passed through a short silica gel column using THF as eluent. After the solvent was removed, the residue was purified by silica gel column chromatography. The products were recrystallized from CH₂Cl₂ and *n*-hexane. Unless otherwise noted, all reactions were performed according to this typical procedure.

4-tert-Butylphenoxy[2,3,7,8,12,13-hexaphenylsubporphyrinato]boron(III) (2a): The residue was purified by column chromatography on silica gel (1:20 mixture of ethyl acetate/*n*-hexane) to give the target compound as a red solid (6.0 mg, 35%). ¹H NMR (600 MHz, CDCl₃): δ = 7.89 (m, 12H; Ph), 7.41 (m, 18H; Ph), 6.85 (d, *J* = 8.6 Hz, 2H; H^{3',5'}), 5.34 (d, *J* = 8.6 Hz, 2H; H^{2',6'}), 1.11 ppm (s, 9H; *t*Bu); ¹³C NMR (150 MHz, CDCl₃): δ = 157.0, 150.8, 143.1, 133.7, 131.9, 131.5, 128.5, 128.3, 126.0, 117.1, 34.0, 31.5 ppm; ¹¹B NMR (192 MHz, CDCl₃): δ = -15.98 ppm; UV/Vis (CHCl₃): λ (ε) = 250 (44000), 304 (40000), 395 (32000), 539 nm (52000 M⁻¹ cm⁻¹); fluorescence (CHCl₃): λ_{ex} = 500 nm; λ_{max} = 563 nm; Φ_F = 0.008; HRMS (ESI-TOF, +): *m/z* calcd for C₅₈H₄₄BN₆O: 851.3674 [M+H]⁺; found: 851.3651.

4-tert-Butylphenoxy[2,3,7,8,12,13-hexa(4-methoxyphenyl)subporphyrinato] boron(III) (2b): The residue was purified by column chromatography on silica gel (10:10:1 mixture of CH₂Cl₂/*n*-hexane/Et₂O) to give the target compound as violet crystals (7.6 mg, 37%). Single crystals suitable for X-ray diffraction analysis were obtained by vapor diffusion of octane into its 1,2-dichloroethane solution. ¹H NMR (600 MHz, CDCl₃): δ = 7.79 (d, *J* = 8.2 Hz, 12H; H^{2',6'}), 6.92 (d, *J* = 8.2 Hz, 12H; H^{3',5'}), 6.81 (d, *J* = 8.6 Hz, 2H; H^{3',5'}), 5.30 (d, *J* = 8.6 Hz, 2H; H^{2',6'}), 3.88 (s, 18H; -OMe) and 1.09 ppm (s, 9H; *t*Bu); ¹³C NMR (150 MHz, CDCl₃): δ = 159.9, 156.8, 151.0, 142.8, 132.7, 132.3, 125.9, 124.6, 117.0, 114.2, 55.4, 33.9, 31.5 ppm; ¹¹B NMR (192 MHz, CDCl₃): δ = -16.05 ppm; UV/Vis (CHCl₃): λ (ε) = 271 (59000), 434 (39000), 553 nm (44000 M⁻¹ cm⁻¹); fluorescence (CHCl₃): λ_{ex} = 515 nm; λ_{max} = 612 nm, Φ_F = 0.026; HRMS (ESI-TOF, +): *m/z* calcd for C₆₄H₅₆BN₆O₇: 1031.4308 [M+H]⁺; found: 1031.4290.

4-tert-Butylphenoxy[2,3,7,8,12,13-hexa(4-methylthiophenyl)subporphyrinato] boron(III) (2c): The residue was purified by column chromatography on silica gel (10:30:1 mixture of CH₂Cl₂/*n*-hexane/Et₂O) to give the target compound as a purple solid (7.7 mg, 34%). ¹H NMR (600 MHz, CDCl₃): δ = 7.80 (d, *J* = 7.8 Hz, 12H; H^{2',6'}), 7.28 (d, *J* = 7.8 Hz, 12H; H^{3',5'}), 6.83 (d, *J* = 8.6 Hz, 2H; H^{3',5'}), 5.31 (d, *J* = 8.6 Hz, 2H; H^{2',6'}), 2.56 (s, 18H; -SMe) and 1.10 ppm (s, 9H; *t*Bu); ¹³C NMR (150 MHz, CDCl₃): δ = 156.6, 150.8, 143.0, 139.8, 132.7, 131.6, 128.3, 126.0, 125.9, 116.9, 33.9, 31.5, 15.4 ppm; ¹¹B NMR (192 MHz, CDCl₃): δ = -16.14 ppm; UV/Vis (CHCl₃): λ (ε) = 287 (87000), 454 (45000), 560 nm (50000 M⁻¹ cm⁻¹); fluorescence (CHCl₃): λ_{ex} = 520 nm; λ_{max} = 654 nm; Φ_F = 0.033; HRMS (ESI-TOF, +): *m/z* calcd for C₆₄H₅₆BN₆OS₆ [M+H]⁺ 1127.2938; found: 1127.2935.

4-tert-Butylphenoxy[2,3,7,8,12,13-hexa(4-dimethylaminophenyl) subporphyrinato]boron(III) (2d): The reaction was performed at room temperature for 5 days under N₂ atmosphere. The reaction mixture was passed through a short silica gel column using THF as eluent. After the solvent was removed, the residue was purified by column chromatography on silica gel (10:5:1 mixture of CH₂Cl₂/*n*-hexane/ethyl acetate) to give the target compound as violet crystals (5.1 mg, 23%). ¹H NMR (600 MHz, CDCl₃): δ = 7.92 (d, *J* = 8.8 Hz, 12H; H^{2',6'}), 6.80 (d, *J* = 8.6 Hz, 2H; H^{3',5'}), 6.78 (d, *J* = 8.8 Hz, 12H; H^{3',5'}), 5.36 (d, *J* = 8.6 Hz, 2H; H^{2',6'}), 3.04 (s, 36H; -NMe₂), 1.09 ppm (s, 9H; *t*Bu); ¹³C NMR (150 MHz, CDCl₃): δ = 157.0, 151.6, 150.1, 142.1, 132.3, 131.4, 125.7, 121.2, 117.0, 112.3, 40.6, 33.9, 31.5 ppm; ¹¹B NMR (192 MHz, CDCl₃): δ = -15.69 ppm; UV/Vis (CHCl₃): λ (ε) = 296 (93000), 503 (53000), 570 nm (42000 M⁻¹ cm⁻¹); fluorescence (CHCl₃): λ_{ex} = 570 nm; λ_{max} = 765 nm, Φ_F = 0.003; HRMS (ESI-TOF, +): *m/z* calcd for C₇₀H₇₄BN₁₂O: 1109.6207 [M+H]⁺; found: 1109.6159.

4-tert-Butylphenoxy[2,3,7,8,12,13-hexa(4-nitrophenyl)subporphyrinato] boron(III) (2e): The residue was purified by column chromatography on silica gel (10:10:1 mixture of CH₂Cl₂/*n*-hexane/Et₂O) to give the target compound as a red solid (4.5 mg, 20%). ¹H NMR (600 MHz, CDCl₃): δ =

8.36 (d, *J* = 8.7 Hz, 12H; H^{3',5'}), 7.99 (d, *J* = 8.7 Hz, 12H; H^{2',6'}), 6.90 (d, *J* = 8.6 Hz, 2H; H^{3',5'}), 5.32 (d, *J* = 8.6 Hz, 2H; H^{2',6'}), 1.11 ppm (s, 9H; *t*Bu); ¹³C NMR (150 MHz, CDCl₃): δ = 156.4, 149.8, 148.5, 144.6, 136.7, 133.6, 132.1, 126.3, 124.5, 117.1, 34.1, 31.5 ppm. ¹¹B NMR (192 MHz, CDCl₃): δ = -16.18 ppm; UV/Vis (CHCl₃): λ (ε) = 297 (61000), 386 (34000), 547 nm (57000 M⁻¹ cm⁻¹); fluorescence (CHCl₃): λ_{ex} = 510 nm; λ_{max} = 581 nm, Φ_F = 0.001; HRMS (ESI-TOF, +): *m/z* calcd for C₅₈H₃₈BN₁₂O₁₃: 1121.2778 [M+H]⁺; found: 1121.2750.

4-tert-Butylphenoxy[2,3,7,8,12,13-hexa(4-trifluoromethylphenyl) subporphyrinato]boron(III) (2f): The residue was purified by column chromatography on silica gel (10:40:1 mixture of CH₂Cl₂/*n*-hexane/Et₂O) to give the target compound as a red solid (7.0 mg, 28%). ¹H NMR (600 MHz, CDCl₃): δ = 7.95 (d, *J* = 8.3 Hz, 12H; H^{3',5'}), 7.74 (d, *J* = 8.3 Hz, 12H; H^{2',6'}), 6.88 (d, *J* = 8.6 Hz, 2H; H^{3',5'}), 5.33 (d, *J* = 8.6 Hz, 2H; H^{2',6'}), 1.12 ppm (s, 9H; *t*Bu); ¹³C NMR (150 MHz, CDCl₃): δ = 156.6, 150.2, 144.1, 134.5, 133.6, 131.6, 131.2, 126.1, 126.0, 125.9, 117.1, 34.1, 31.8 ppm; ¹¹B NMR (192 MHz, CDCl₃): δ = -16.14 ppm. ¹⁹F NMR (565 MHz, CDCl₃): δ = -62.62 ppm; UV/Vis (CHCl₃): λ (ε) = 252 (47000), 308 (43000), 384 (30000) and 538 nm (57000 M⁻¹ cm⁻¹); fluorescence (CHCl₃): λ_{ex} = 500 nm; λ_{max} = 564 nm; Φ_F = 0.001; HRMS (ESI-TOF, +): *m/z* calcd for C₆₄H₃₈BF₁₈N₆O: 1259.2918 [M+H]⁺; found: 1259.2908.

4-tert-Butylphenoxy[2,3,7,8,12,13-hexa(4-methoxycarbonylphenyl) subporphyrinato]boron(III) (2g): The residue was purified by column chromatography on silica gel (20:1 mixture of CH₂Cl₂/Et₂O) to give the target compound as a red solid (10.3 mg, 43%). ¹H NMR (600 MHz, CDCl₃): δ = 8.11 (d, *J* = 8.3 Hz, 12H; H^{2',6'}), 7.90 (d, *J* = 8.3 Hz, 12H; H^{2',6'}), 6.87 (d, *J* = 8.6 Hz, 2H; H^{3',5'}), 5.34 (d, *J* = 8.6 Hz, 2H; H^{2',6'}), 3.98 (s, 18H; -COOMe), 1.12 ppm (s, 9H; *t*Bu); ¹³C NMR (150 MHz, CDCl₃): δ = 166.8, 156.6, 150.3, 143.8, 135.7, 133.9, 131.3, 130.6, 130.1, 129.1, 117.1, 52.5, 34.0, 31.5 ppm; ¹¹B NMR (192 MHz, CDCl₃): δ = -16.10 ppm; UV/Vis (CHCl₃): λ (ε) = 276 (68000), 312 (50000), 394 (34000), 545 nm (58000 M⁻¹ cm⁻¹); fluorescence (CHCl₃): λ_{ex} = 500 nm; λ_{max} = 574 nm; Φ_F = 0.003; HRMS (ESI-TOF, +) calcd for C₇₀H₅₆BN₆O₁₃: *m/z* calcd for 1199.4004 [M+H]⁺; found: 1199.3977.

Acknowledgements

Support is acknowledged from the Spanish MICINN (CTQ2011-24187/BQU and the CONSOLIDER INGENIO 2010, CSD2007-00010 on Molecular Nanoscience) and the CAM (MADRISOLAR-2, S2009/PPQ/1533). This work was also supported by Grants-in-Aid (No. 22245006 (A) and 20108001 “pi-Space”) for Scientific Research from MEXT. T.H. acknowledges a JSPS Fellowship for Young Scientists.

- a) M. S. Rodríguez-Morgade, S. Esperanza, T. Torres, J. Barberá, *Chem. Eur. J.* **2005**, *11*, 354–360; b) J. R. Stork, J. J. Brewer, T. Fukuda, J. P. Fitzgerald, G. T. Yee, A. Y. Nazarenko, N. Kobayashi, W. S. Durfee, *Inorg. Chem.* **2006**, *45*, 6148–6151; c) G. M. D. Aminur Rahman, Lüders, M. S. Rodríguez-Morgade, E. Caballero, T. Torres, D. M. Guldi, *ChemSusChem* **2009**, *2*, 330–335.
- a) C. G. Claessens, D. González-Rodríguez, T. Torres, *Chem. Rev.* **2002**, *102*, 835–853; b) N. Kobayashi in *The Porphyrin Handbook, Vol. 15: Synthesis and Spectroscopic Properties of Phthalocyanine Analogs* (Eds.: K. M. Kadish, K. M. Smith, R. Guillard), Academic Press, San Diego, **2003**, pp. 161–262; c) T. Torres, *Angew. Chem.* **2006**, *118*, 2900–2903; *Angew. Chem. Int. Ed.* **2006**, *45*, 2834–2837.
- Y. Rio, M. S. Rodríguez-Morgade, T. Torres, *Org. Biomol. Chem.* **2008**, *6*, 1877–1894.
- S. Shimizu, T. Otaki, Y. Yamazaki, N. Kobayashi, *Chem. Commun.* **2012**, *48*, 4100–4102.
- For recent reviews, see a) Y. Inokuma, A. Osuka, *Dalton Trans.* **2008**, 2517–2526; b) A. Osuka, E. Tsurumaki, T. Tanaka, *Bull. Chem. Soc. Jpn.* **2011**, *84*, 679–697.
- M. Kitano, S.-y. Hayashi, T. Tanaka, H. Yorimitsu, N. Aratani, A. Osuka, *Angew. Chem. Int. Ed.* **2012**, *51*, 5593–5597.

- [7] A. M. Lamsabhi, M. Yáñez, O. Mó, C. Trujillo, F. Blanco, I. Alkorta, J. Elguero, E. Caballero, M. S. Rodríguez-Morgade, C. G. Claessens, T. Torres, *J. Porphyrins Phthalocyanines* **2011**, *15*, 1220–1230.
- [8] In general, bisaryl maleonitrile precursors **4** are not readily accessible because the thermodynamically more favored fumaronitrile isomers **3** are often main or sometimes exclusive products (see the Supporting Information, Scheme S1). Attempts to photoisomerize the fumaronitriles **3** into the corresponding maleonitriles **4** gave inseparable mixtures of these *Z* isomers and phenanthrene-9,10-dicarbonitriles **6**, as well as their 4a,4b-dihydro derivatives **5**. The phenanthrene derivatives **5** and **6** arise from a photochemically driven, 6 π -electron electrocyclic reaction involving the olefinic double bond and one double bond of each benzene ring. See, for example: a) H.-C. Yeh, W.-C. Wu, Y.-S. Wen, D.-C. Dai, J.-K. Wang, C.-T. Chen, *J. Org. Chem.* **2004**, *69*, 6455–6462; b) F. B. Mallory, C. W. Mallory, *Organic Reactions*, Vol. 30, Wiley, Hoboken, **1984**, Chapter 1, pp. 1–456.
- [9] L. S. Liebeskind, J. Srogl, *Org. Lett.* **2002**, *4*, 979–981.
- [10] M. S. Rodríguez-Morgade, C. G. Claessens, A. Medina, D. González-Rodríguez, E. Gutierrez-Puebla, A. Monge, I. Alkorta, J. Elguero, T. Torres, *Chem. Eur. J.* **2008**, *14*, 1342–1350.
- [11] Y. Inokuma, Z. S. Yoon, D. Kim, A. Osuka, *J. Am. Chem. Soc.* **2007**, *129*, 4747–4761.
- [12] E. Caballero, J. Fernández-Ariza, V. M. Lynch, C. Romero-Nieto, M. S. Rodríguez-Morgade, J. L. Sessler, D. M. Guldi, T. Torres, *Angew. Chem. Int. Ed.* **2012**, *51*, 11337–11342.
- [13] D. Dini, S. Vagin, M. Hanack, V. Amendola, M. Meneghetti, *Chem. Commun.* **2005**, 3796–3798.
- [14] M. Geyer, F. Plenzig, J. Rauschnabel, M. Hanack, B. del Rey, A. Sastre, T. Torres, *Synthesis* **1996**, 1139–1151.
- [15] a) N. Kobayashi in *meso-Azaporphyrins and their Analogues in The Porphyrin Handbook*, Vol. 13 (Eds.: K. M. Kadish, K. M. Smith, R. Guillard), Academic Press, San Diego, **2003**, pp. 301–359; b) T. Goslinski, E. Tykarska, M. Kryjewski, T. Osmalek, S. Sobiak, M. Gdaniec, Z. Dutkiewicz, J. Mielcarek, *Anal. Sci.* **2011**, *27*, 511–515.
- [16] CCDC-921609 (**2b**) contains the supplementary crystallographic data for this paper. These data can be obtained free of charge from The Cambridge Crystallographic Data Centre via www.ccdc.cam.ac.uk/data_request/cif.
- [17] E. Tsurumaki, Y. Inokuma, S. Easwaramoorthi, J. M. Lim, D. Kim, A. Osuka, *Chem. Eur. J.* **2009**, *15*, 237–247.
- [18] a) H. Miwa, K. Ishii, N. Kobayashi, *Chem. Eur. J.* **2004**, *10*, 4422–4435; b) E. A. Ougha, K. A. M. Crebera, M. J. Stillman, *Inorg. Chim. Acta* **1996**, *246*, 361–369.
- [19] C. Hansch, A. Leo, R. W. Taft, *Chem. Rev.* **1991**, *91*, 165–195.
- [20] A partially chemically reversible oxidation implies that the oxidized species formed after an electron transfer reacts in solution, but with a low *k*. In CV, this is reflected by a wave composed of a normal anodic peak and a less intense, but still visible cathodic peak, as shown in Figure 3 for **2a**, **b**, **e**, **f**, and **g**. Because the chemical reaction is slow, usually the i_{pc}/i_{pa} ratio increases by increasing the scan rate when doing the CV. This is illustrated in Figure S10 in the Supporting Information by performing CV experiments using a scan rate of 0.1–0.2 V s⁻¹ versus the scan rate of 0.05 V s⁻¹ used in voltammograms depicted in Figure 3.
- [21] a) D. Larumbe, M. Moreno, I. Gallardo, J. Bertran Cl. P. Andrieux, *J. Chem. Soc. Perkin Trans. 2* **1991**, 1437–1443; b) M. Kádár, Z. Nagy, T. Karancsi, G. Farsang, *Electrochim. Acta* **2001**, *46*, 1297–1306.

Received: March 25, 2013
Published online: June 19, 2013